

P6.3 THE CONTRIBUTION OF COASTAL AEROSOL FROM BREAKING WAVES TO VISIBLE AND IR LIGHT-EXTINCTION OVER A 10KM OPTICAL PATH DURING RED

Antony Clarke*, V. Kapustin, S. Howell, K. Moore,
Department of Oceanography, University of Hawaii, 1000 Pope Rd. Honolulu, HI 96822

1. INTRODUCTION

The Rough Evaporation Duct (RED) experiment was carried out off the NE coast of Oahu, Hawaii in August-September of 2001. RED was conceived with the intention of improving prediction of electro-optic (EO) signal propagation over a wind-roughened sea. This requires knowledge of its interaction with the sea surface, the mean profiles of humidity, temperature, wind and their turbulent fluctuations. It also requires an assessment of the interaction of EO propagation with near surface aerosol. This is particularly true in conditions of high sea-state or in coastal environments when breaking waves can generate elevated concentrations of near surface marine aerosol. Here we will use coastal aerosol measurements under breaking wave conditions to estimate the contribution of coastal breaking waves to the RED EO extinction.

1.1 MEASUREMENT DESCRIPTION

A 10km EO path between the R/V FLIP anchored off the coast and a receiver on the coast

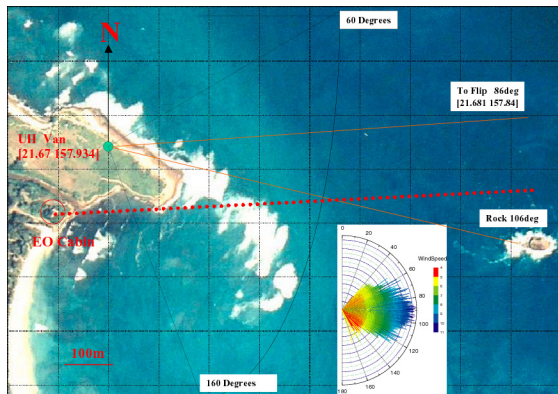


Figure 1. View of the coastal measurement site including the EO cabin, UH sampling van location, breaking wave region and directions to FLIP. Note wind speed/direction insert shows that EO path is generally exposed to sea-salt plumes from breaking waves (usually 85-120deg at 4-7ms⁻¹).

passed over a near shore region of frequent breaking waves about 500m in front of the detector (Figure 1) located in the EO cabin on the shore. Marine aerosol produced from these breaking waves varied in intensity of production and in the degree to which it intercepted the EO path depending upon environmental factors including wind direction.



Figure 2. View from the coastal site including the EO detector and the UH aerosol sampling van.

Because the EO path was designed to pass only about 3-4 m above the surface these aerosol usually intercepted the EO path over some distance.

* Corresponding author address: Antony Clarke,
Department of Oceanography, University of Hawaii,
1000 Pope Rd. Honolulu, HI 96822;
e-mail: tclarke@soest.hawaii.edu

Our UH aerosol research van (UHV) was located about 400m toward FLIP from the EO detector and about 150m north of the EO path (Figure 2a,b). It was located at a coastal section where the closest near-shore breaking waves seldom experienced conditions that allowed them to enter our 13m high UHV inlet. This meant the UHV usually sampled open-ocean aerosol unless more southerly winds brought aerosol from the breaking wave region upwind of the EO detector. The latter cases had far higher extinction values, allowing us to characterize the influence of these waves upon the RED EO path extinction. Analysis of the coastal geometry and the wind speeds were then used to estimate the impact of both the open ocean aerosol and the contributions of aerosol from breaking waves upon the 10km EO signal.

The UHV sample inlet terminated inside the portable laboratory van. Several smaller tubes were mounted near the center of the PVC sample line flow with diameters selected to allow for near isokinetic sampling to various instruments. The largest flow of 30 lpm went to a three-wavelength integrating nephelometer (Mod. 3551 TSI Inc.) that alternately inserted an impactor with aerodynamic size cut at 1 μm . This generally operated near 55% relative humidity compared to ambient values that were usually in the 70-85% range. Truncation corrections for all nephelometer data were made after Anderson and Ogren (1998). Two condensation nuclei, CN, counters recorded particle number concentrations at 40°C (CNcold) and 360°C (CNhot). Refractory particles remaining after heating to 360°C, such as sea salt, could be distinguished from more volatile species such as sulfates at up to 1Hz time resolution. This afforded rapid assessment of the variability in breaking wave events. Other supportive measurements included wind speed, wind direction, relative humidity, precipitation, tides, pressure, sunlight and meteorological parameters.

Size distributions were determined with an aerosol particle spectrometer (APS Mod. 3320, TSI Inc.; $0.5 < D_p < 10 \mu\text{m}$), radial differential mobility analyzer (RDMA; $0.007 < D_p < 0.3 \mu\text{m}$) [Zhang et al., 1985] and a laser optical particle counter (OPC; $0.1 < D_p < 7 \mu\text{m}$). Both of the latter employed thermal volatility to measure distributions in air sampled at 40, 150 and 300°C. This established the volatile particle fractions (Clarke et al., 1991) and isolated the sea-salt distribution refractory at 360°C. The RDMA was used in conjunction with a LAG (Lagged Aerosol Grab) chamber (Clarke et al., 1998) that “captured” a sample of air over about 15s for subsequent analysis over several minutes at three temperatures. This ensured that small-scale temporal variation in the sample did not occur during the 3 min measurement period, a critical requirement to sample wave breaking plumes of 15-60s duration. The sample mast was also removed for a period to get the near surface size-distributions at 3m altitude and concurrent extinction data for interpretation of aerosol gradients for the near surface EO path.

2. SAMPLING ISSUES

Quantitative comparisons of independently measured and remotely sensed properties require proper calibrations, corrections and transformations to measurement conditions. The change in marine aerosol size with relative humidity (RH) is one issue that affects many physical, chemical and optical properties examined in RED. Water uptake influences aerosol size, density and refractive index in ways that impact the interpretation of data from various instruments and its extrapolation to ambient conditions. Some sizing instruments are nominally “dry” in the sense that they measured at low (but often different) RH with relatively little water volume associated with them. Other instruments (eg. nephelometers) were at intermediate humidity. The DMA, OPC and APS size distributions were measured at instrument RH. The DMA employed desiccated sheath air sample flow to bring RH to about 25% for sizing. The OPC mixed sample and desiccated air upstream of the instrument to lower RH to about 40%. Obtaining size distributions from these instruments generally require explicit corrections for a) measured vs. calibration aerosol properties, b) measured vs. desired humidity conditions, c) size dependent instrument performance and d) size dependent sampling. The combined DMA, OPC and APS distributions yielded a composite distribution at 40%RH with uniform logD scale of 50 diameter steps per decade and 167 diameters altogether. Growth from 40% to ambient RH was then applied to combined size distributions using $g(\text{RH})$ for marine aerosol (Swietlicki et al., 2000)

2.4 Inlet losses

Aerosol sampling systems also often lose particles over certain size ranges as a result of diffusion, inlet configuration, anisokinetic sampling, sedimentation, impaction etc. These latter effects are often greatest for large particles. Because breaking waves often generate large particles that can affect aerosol optics (Reid et al., 2001, De Leeuw et al., 2000; Vignati et al., 2001) we expect losses for larger sizes in our inlet system. Losses were estimated here based upon results of our earlier SEAS study in Hawaii (Clarke et al., 2002) and used to correct and interpret coarse particle data obtained from our sampling system during RED.

3. OBSERVATIONS

3.1 Representative UH Van Data and Aerosol Microphysics

Measured light scattering reflects variations in aerosol concentrations or size. A four-hour time series of measurements at 13 m asl under variable wind speed and direction are shown in Figure 3. Time periods when winds favored open ocean values have more stable scattering values about a factor of 4

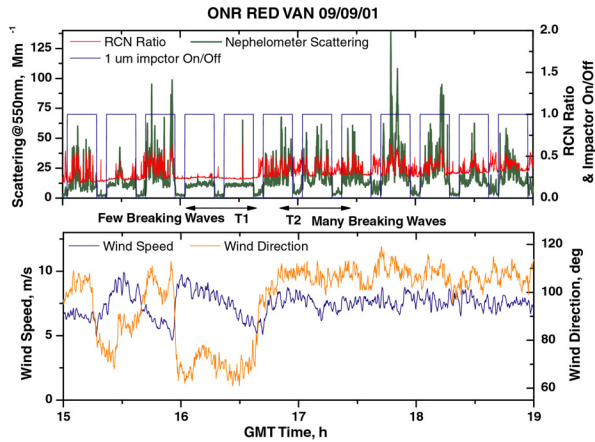


Figure 3a shows an example of light scattering (550nm) from mast at 13m cycled with and without a 1μm impactor over a 6 h hour period along with associated excursions in wind speed and direction.

lower than periods when winds blew over breaking waves. Aerosol light scattering (corrected for truncation errors) is also interrupted by a 5min period when the impactor [1μm aerodynamic cut size] is inserted into the flow to reveal the submicrometer scattering data. These impactor data also show that shoreline waves enhance measured scattering at 13m compared to open ocean data.

Variation in light scattering can be a result of fluctuations in wind direction (exposure to breaking waves), wind speed (dilution of breaking wave plumes), tidal variations (variations in breaking waves due to depth changes) etc. Measurements at 13m for the UHV are shown in Figure 4 as a function of wind direction and tides along with concurrent scattering

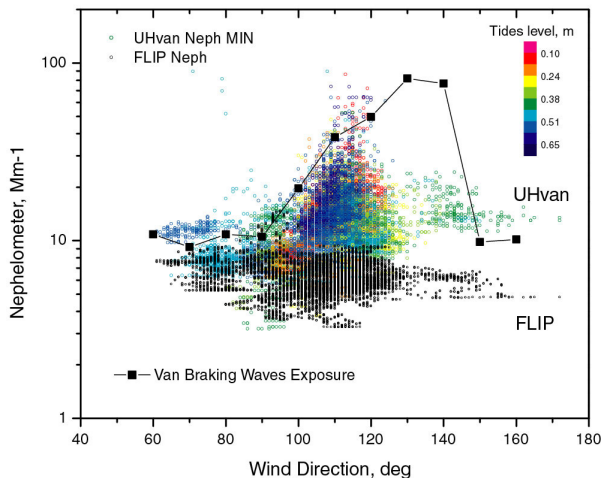


Figure 4 Variations in scattering with wind direction and tides as measured at 13m from the UHV (color). Concurrent data from FLIP (black) suggests reveals enhancements at 13m from coastal breaking waves.

data measured at FLIP which was also exposed to virtually identical winds (not shown). A clear enhancement relative to FLIP of about a factor of 2-8 is evident for directions that bring air over the breaking waves SE (100-120 deg) of the UHV (see Figure 1). An “exposure” index is also shown for the UHV that is an estimated relative enhancement based upon the anticipated increased path over breaking waves expected upwind of the van for various wind directions. A similar index was also prepared for the EO cabin (not shown). This differs from that of the UHV primarily in wind direction due to the different orientation of the cabin to the wave breaking region (see Figure 1). This exposure index does coincide with the observed enhancements in scattering. Since wind directions seldom exceeded 130deg there are few data points in that region.

Although the 13m data shown above reveals a breaking wave enhancement the actual EO propagation between FLIP and the EO cabin (Figure 1) occurred at about 4 m. In order to investigate the effect of a vertical gradient in aerosol in the lowest several meters we carried out measurements with and without the UHV sample inlet to provide data at about 4m and 13m asl from 0-4hrs GMT on September 10. The results of this test for a period when winds were blowing over the breaking waves at about 90 deg toward the UHV are shown in Figure 5 along with the dramatic changes in the size distributions. These distributions are as measured and require corrections for coarse particle losses and RH growth before being used to calculate optical properties. Also shown are concurrent nephelometer values measured on FLIP that are similar to the loss corrected (see below) UHV data at 13 m. UHV data at 4m are an order of magnitude higher than at 13m revealing the strong near surface gradient in concentration. If a logarithmic profile is assumed for near surface concentrations then these data would suggest a further enhancement of 20% at 3m and 40% enhancement at 2m compared to our measured 4m UHV data.

However, actual concentrations over the breaking waves about 200-400m upwind are expected to be even higher than those measured at the UHV since they will not be depleted by fallout of larger particles or dilution through mixing. This has been demonstrated with lidar data collected during our earlier coastal experiments at Bellows Air Force Station (BAFS) (Porter et al., 2002). This data was obtained as part of our Shoreline Environment Aerosol Study (SEAS) experiment carried out about 30km south along the same coast as the RED experiment. Aerosol extinction inferred from lidar data (Porter et al., 2000) was validated with aerosol measurements during SEAS (Clarke et al., submitted JAOT). As a result we can estimate the typical decrease in extinction downwind of the breaking waves under similar conditions to these in RED. Assuming a similar fall-off with distance for the RED data allows us to scale our UHV measurements made 200-400m downwind of the breaking waves (see

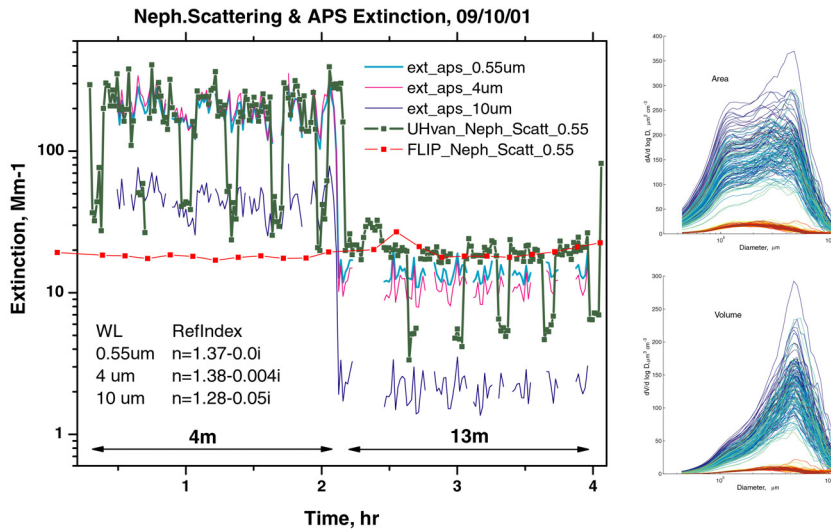


Figure 5. A time series of UHV light scattering (green - 550nm) cycled every 5 min with and without a 1um impactor during a 4 hour period with winds over breaking waves. The first 2 hours are 4m data followed by 2 hours of 13m data. Concurrent open ocean values from FLIP (red) are close to 13m values. Other lines are extinction values calculated from size for indicated wavelengths. Panels on right show size distributions of aerosol surface area (top) and volume (bottom) for both altitudes.

Figure 1) by the relative lidar gradient observed in SEAS. These lidar data suggest about factor of 3 or so in extinction over our ambient UHV values can be expected above the wave region.

3.3 Size Distributions

The measurements made above were for “dry” aerosol sizes as measured without correction for RH. Because RH has such a significant effect on marine aerosol size we generally operate instruments such as the DMA and OPC in the “dry” mode at less than 40% RH so that sizes and refractive indices are close to dry mass properties. Then, as described earlier, appropriate ancillary information is used to “grow” particles to larger sizes at a given humidity. Before comparing measured size distributions to other measurements (eg. SEAS lidar) it is important to evaluate size data by testing it against concurrently measured optical data (eg. nephelometer light scattering). This constitutes a “local closure” by using the combined size distribution, size resolved chemistry and associated refractive indices to model aerosol light scattering at the nephelometer RH using the same tower inlet system. If the resulting calculated scattering and the wavelength dependence expressed by the Angstrom exponent agree with values measured by the nephelometer then our physio-chemical description of the aerosol is appropriate for related optical properties.

3.4 Aerosol Optics and Size-Distributions

The total measured size distribution at nephelometer RH has been used to model expected scattering extinction for RH in the UH and UW nephelometers including correction for the different transmission efficiency of the UW inlet system. Particle diameter growth resulting from changes in RH [eg. $D(\text{nephelometer RH}) / D(\text{measured RH})$] must be

considered (Swietliki et al., 2000) for the clean marine submicrometer mode and for sea-salt (Tang, 1997). This growth to ambient sizes is associated with refractive index changes that also impact the calculated scattering. In brief, our approach to establishing ambient scattering is to measure the ‘dry’ size, correct them to nephelometer RH and compare calculated and measured scattering (closure), apply losses for inlet system, grow aerosol to ambient sizes, estimate scattering lost due to large particles not entering inlet and calculate ambient size distributions and scattering.

Additional corrections to estimate aerosol present in EO path involves scaling our data to anticipated values over breaking waves based upon our estimated vertical gradient and the near-surface horizontal gradient for calibrated lidar extinction measured over similar coastal breaking waves. Anticipated impacts on EO extinction measured at the EO cabin are then dependent upon wind direction and the “exposure” index mentioned earlier. The assessments based upon the size distributions corrected for losses and RH also allows us to calculate effects at other wavelengths such as the 4μm near IR values used for the EO measurements. This approach has been used to generate the estimated effects of reef aerosol on the 10km EO extinction between FLIP and the EO cabin.

The results of this preliminary assessment are shown in the Table inset below. Exposure to breaking wave plumes is given two ranges. Low or 250 m is estimated as a reasonable value for the surf exposure for the EO cabin if winds are not blowing from the offshore rock (Fig. 1) while 1000 m would be a maximum value for directly downwind of the rock with very active surf. A factor of two has also been used to bound the anticipated range of scattering values at 4 m above the waves for the three wavelengths shown in the upper panel. These values are

Expected Near-surface Range in Extinction Values [Mm-1] above breaking waves. :			
Open Ocean	0.55um =20	4um= 12	10um=2
13 m Breaking Waves	0.55um = 20-60	4um= 12-36	10um=2-6
4 m Breaking Waves	0.55um = 330-660	4um= 330-660	10um=75-150

Approximate Reduction in Transmittance to FLIP at 10km Including Coastal Aerosol for EO transmission 4 masl at 0.55um, 4um and 10um for low wave height case. Effects Could double or more for higher waves and lower winds (less dilution). [R.F. = Reduction Factor compared to open ocean transmittance]

Estimated Range in Extinction at 4 m for Breaking Waves
0.55um = 330-660 Mm-1 4um = 330-660 Mm-1 10um = 75-150 Mm-1

Exposure(m)	0.55um	R.F.	4.0um	R.F.	10um	R.F.
N=(no waves)	19 %	1	12%	1	2%	1
250m (Low?)	24 –30 %	1.3 –1.7	18 -25 %	1.6 –2.2	3.8 -5.5 %	1.9 –2.8
1000m (Max.)	40 -57 %	2.2 –3.1	35 -54 %	3.1 - 4.7	9 –16 %	4.5 –7.8

estimated based upon discussions above but variability in gradients, sea state, wind speeds and directions etc. will have significant influences on actual values. Here the objective is to assess the potential for influencing the EO transmission over the 10 km to FLIP.

In the bottom Table above we have taken the extinction values from the upper Table and estimated the change in EO transmission for 0.55, 4.0 and 10 μm wavelengths. These are shown for 3 cases: 1) without coastal breaking wave aerosol, 2) with 250 m exposure to waves and 3) 1,000 m exposure to waves. The percent reductions in transmission are based upon Beer's law extinction for the ambient aerosol over the 10 km path between FLIP and the EO cabin. The reduction factor (RF) values shown are the ratio of the estimated extinction to the nominal open ocean extinction. The range of values indicate the effect of the estimated extinction values shown in the upper Table.

Summary

We have taken aerosol size-distributions and light scattering data collected during RED at 4 m and 13 m altitudes and extracted the contributions due to breaking waves. These have been used to develop estimates of the impact of near shore breaking waves on measured EO extinction between FLIP and the coastal EO site. This preliminary assessment indicates that significant effects on EO extinction appear probable due to aerosol from the coast breaking waves at both 0.55 and 4.0 μm wavelengths with much smaller percentage changes in the 10 μm wavelength. However, the relative effect (RF value) compared to open-ocean transmission is greatest for the 10 μm wavelength suggesting that under more extreme aerosol production from breaking waves EO

transmission at this wavelength could also be significantly affected. Since the combination of processes at work in this environment can result in large inhomogeneous plumes and rapid variability it appears like that rapid fluctuations observed in EO signals at 4.0 μm can be expected due to these coastal aerosol.

We hope to integrate this assessment with variations in wind directions, wind speed, tides and sea-state to estimate temporal variations in the EO signal. Comparisons with the measured EO signal could then be made to see if measured variations show any indications of these predicted effects.

Acknowledgements:

We extend special appreciation for Drs. R. Ferek and S. Ackleson of the Office of Naval Research for their support [N00014-96-1-0320] of our long-term measurements at BAFS and for the RED experiment described here.

REFERENCES

- Anderson, T. L. and J.A. Ogren, Determining aerosol radiative properties using the TSI 3563 integrating nephelometer, *Aerosol. Sci. Technol.*, 29, 57-69, (1998)
- Clarke, A.. and V. Kapustin, The Shoreline Environment Aerosol Study (SEAS-2000): Marine aerosol measurements influenced by a coastal environment and long range transport, *J.Atmos.Ocean.Technol.*, submitted 2002.
- Clarke, A. D. "A Thermo-optic Technique for in-situ Analysis of Size-resolved Aerosol Physicochemistry", *Atmos. Env.*, 25A, ¼, 635-644, 1991.

- de Leeuw, G., F. Neele, M. Hill, M. Smith and E. Vignati, Production of sea-spray aerosol in the surf zone, *J. Geophys. Res.*, 29,397-29,409, 2000.
- Lienert, B.R., J. N. Porter, and S.K. Sharma, *Marine Geodesy*, 22, pp. 259-265, 1999.
- Porter, J.N., B. Lienert, and S.K. Sharma, Using the horizontal and slant lidar calibration methods to obtain aerosol scattering coefficients from a coastal lidar in Hawaii, *J. Atmos. Ocean. Tech.*, 17(11), 1445-1454, 2000).
- Porter J.N., S.K. Sharma, B. R. Lienert, and Eric Lau, Aerosol Scattering Fields Over Bellows Beach, Oahu During the SEAS Experiment (*J. Atmos. Ocean. Tech.*, submitted 2002)
- Reid, J.S., H. Jonsson, M. Smith, and A. Smirnov, Evolution of the vertical profile and flux of large sea-salt particles in a coastal zone, *J. Geophys. Res.*, 106, 12,039-12,053, 2001.
- Swietlicki, E., J. Zhou, D.S. Covert, K. Hämeri, B. Busch, M. Väkevä, U. Dusek, O.H. Berg, A. Wiedensohler, P. Aalto, J. Mäkelä, B.G. Martinsson, G. Papaspiropoulos, B. Mentes, G. Frank, and F. Stratmann (2000), Hygroscopic properties of aerosol particles in the north-eastern Atlantic during ACE-2, *Tellus*, 52B, 201-227.
- Tang, I.N., A.C. Tridico, and K.H. Fung (1997), Thermodynamic and optical properties of sea salt aerosol, *J. Geophys. Res.*, 102, 23269 – 23275.
- Vignati, E, G. de Leeuw, R. Berkowicz, Modeling coastal aerosol transport and effects of surf produced aerosol on processes in the marine boundary layer; *J. Geophys. Res.*, 106, 20,225-20,238, 2001.
- Zhang, S. H., Y. Akutsu, L. M. Russell, R. C. Flagan, and J. H. Seinfeld, Radial Differential Mobility Analyzer, *Aerosol Sci. Technol.*, 23, 357-371, 1995.